Electronic Supplementary Information

Two levels of conformational pre-organization consolidate strong CH hydrogen bonds in chloride-triazolophane complexes

Yuran Hua, Raghunath O. Ramabhadran, Jonathan A. Karty, Krishnan Raghavachari, Amar H. Flood*

Department of Chemistry, Indiana University, 800 East Kirkwood Avenue, Bloomington, IN 47405, USA

Email of corresponding author: aflood@indiana.edu

S.1 GENERAL METHODS

All reagents were obtained from commercial suppliers and used as received unless otherwise noted. 1,3-Diazidopropane (**4**)[S1] and 1-*tert*-butyl-3,5-diethynylbenzene (**5**)[S2] were prepared following literature procedures. Column chromatography was performed on silica gel (160 – 200 mesh), and thin-layer chromatography (TLC) was performed on precoated silica gel plates (0.25 mm thick, 60F254, Merck, Germany) and observed under UV light. Nuclear magnetic resonance (NMR) spectra were recorded on Varian Inova (500 MHz) and Varian Inova (400 MHz) spectrometers at room temperature (298 K). Chemical shifts were referenced to the residual solvent peaks. High resolution electrospray ionization (ESI) mass spectrometry was performed on a Thermo Electron Corporation MAT 95XP-Trap mass spectrometer. Low resolution ESI mass spectrometry was performed on an Agilent 1200/6130 mass spectrometer with loop injection. Melting points were determined with an Electrothermal MEL-TEMP setup.

Safety Comment: Sodium azide is very toxic, personal protection precautions should be taken. As low molecular weight organic azides are potential explosives, care must be taken during their handling. Generally, when the total number of carbon (N_C) plus oxygen (N_O) atoms is less than the total numbers of nitrogen atoms (N_N) by a ratio of three, i.e., (N_C + N_O) / N_N < 3, the compound is considered as an explosive hazard. In those instances, the compound was prepared prior to use and used immediately. A standard PVC blast shield was used when necessary.

S.2 SYNTHESES OF TRIAZOLOPHANE 2

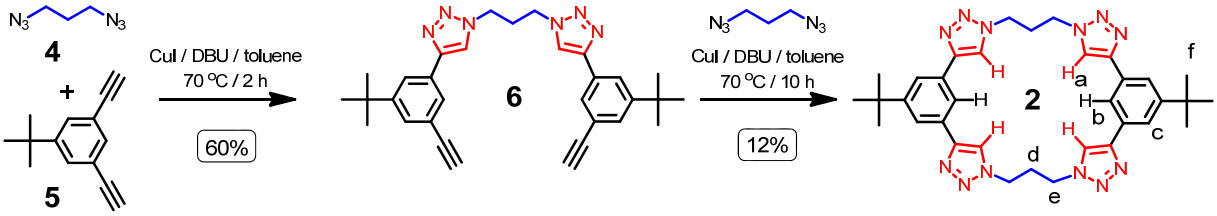

Scheme S1. Syntheses of triazolophane **2**.

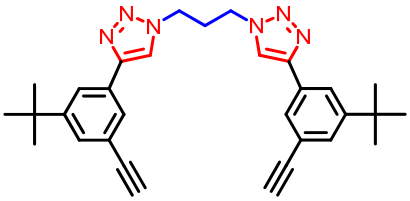

5/8-Oligomer 6: Diazide **4** (25 mg, 0.2 mmol) and diacetylene **5** (450 mg, 2.5 mmol) were dissolved in toluene (50 mL). The mixture was degassed with argon for 10 minutes at 70 ºC, after which CuI (38 mg, 0.2 mmol) was added with a further degassing for 10 min. The reaction was initialized by the injection of 1,8-diaza[5.4.0]bicycloundec-7-ene (DBU) (122 mg, 0.8 mmol). After stirring and degassing for 2 hours at 70 ºC, the volatiles were removed in vacuo

and the dark oil was washed with water (60 ml), extracted with CH_2Cl_2 (2 × 30 ml), dried (Na_2SO_4) and concentrated under reduced pressure. The crude product was purified by column chromatography (SiO_2, 4:1 (*v*/*v*) hexane:acetone) to afford 59 mg of **6** as a pale yellow solid. Yield: 60%. ^{1}H NMR ($CDCl_3$, 400 MHz), δ = 7.94 (t, 2H, *J* = 1.6 Hz), 7.90 (s, 2H), 7.71 (t, 2H, *J* = 1.6 Hz), 7.51 (t, 2H, *J* = 1.6 Hz), 4.47 (t, 4H, *J* = 6.0 Hz), 3.09 (s, 2H), 2.64 (quintet, 2H, *J* = 6.0 Hz), 1.36 (s, 18H). ^{13}C NMR ($CDCl_3$, 100 MHz), δ = 152.2, 147.5, 130.2, 129.1, 126.6, 123.4, 122.3, 120.7, 83.7, 77.0, 46.7, 34.8, 31.1, 30.7. HR-ESI-MS: $C_{13}H_{35}N_6$ $[M + H]^+$, Calculated: 491.2923, Found: 491.2940. Melting point: 67-70 ºC.

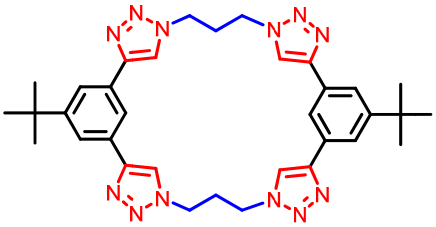

Triazolophane 2: Toluene (300 mL) was placed in a two neck flask and was degassed with argon for 10 minutes at 70 ºC before CuI (96 mg, 0.5 mmol) was added. The mixture was maintained at 70 ºC during the reaction procedure. After further degassing for 10 minutes, DBU (0.99 g, 6.5 mmol) was injected. A solution of 5/8-oligomer **6** (245 mg, 0.5 mmol) and diazide **4** (63 mg, 0.5 mmol) in dry toluene (60 mL) was added dropwise to the solution over 6 h, and the reaction mixture was stirred for another 4 h under argon. The volatiles were then removed in vacuo and the dark oil was purified by column chromatography (SiO_2, 100:3 CH_2Cl_2:MeOH) three times to afford 37 mg of **2** as a white solid. Isolated yield: 12%. ^{1}H NMR (CD_2Cl_2, 400 MHz), δ = 7.65 (s, 2H), 7.40 (s, 4H), 7.23 (s, 4H), 4.61 (t, 8H, *J* = 5.6 Hz), 2.84 (quintet, 4H, *J* = 5.6 Hz), 1.26 (s, 18H). ^{13}C NMR ($CDCl_3$, 100 MHz), δ = 151.7, 148.2, 130.2, 122.0, 120.0, 119.7, 49.1, 31.2, 29.7. HR-ESI-MS: $C_{34}H_{41}N_{12}$ $[M+H]^+$, Calculated: 617.3577, Found: 617.3608. Melting point: >220 ºC.

S.3 ESI-MS OF THE CHLORIDE COMPLEX OF TRIAZOLOPHANE 2

Triazolophane **2** solution (50 μM) containing 1.0 eq. of tetrabutylammonium chloride (TBA^+•Cl^-) in CH_2Cl_2 was prepared. The sample was injected into the ionizer through an empty loop with CH_2Cl_2 as solvent, and detected with negative ion mode. Injection volume: 20 μL; Drying gas temperature: 250 °C; Vaporizing gas temperature: 225 °C; Capillary voltage: 2000 V; Charging voltage: 2000 V; Fragmentor: 45.

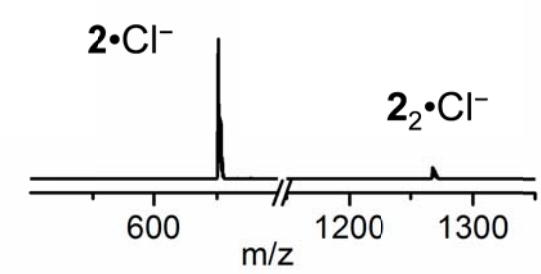

Figure S1. ESI-MS **2** (50 μM) with TBA^+•Cl^- (1.0 eq) in CH_2Cl_2.

S.4 ^{1}H NMR TITRATION OF TRIAZOLOPHANE 2 AND BINDING ENERGY DETERMINATION

Triazolophane **2** solution in 400 μL CD_2Cl_2 at 500 μM was loaded into a capped NMR tube, and the initial spectrum was recorded. Aliquots of tetrabutylammonium chloride ($TBA^+•Cl^–$) solution in CD_2Cl_2 at 20 mM were then added into the NMR tube with a microsyringe through rubber septa. Spectra were recorded after each addition.

Chemical shift migrations of protons a, b, c, d, e (Scheme S1), and the α-methylene proton on tetrabutylammonium cation were modeled by HypNMR2008[S3] with a set of three equilibria (Figure S2)[S4]. $TBA^+•Cl^–$ ion-pair formation was included in the binding model. Literature value of the ion-pair stability ($\Delta G_{TBA+•Cl–} = –27.7$ kJ mol$^{–1}$, $\log K_{ip} = 4.86$)[S5] was used and fixed.

$$\mathbf{2} + Cl^– = \mathbf{2}•Cl^– \qquad K_a \qquad \text{(S1)}$$

$$TBA^+ + Cl^– = TBA^+•Cl^– \qquad K_{ip} \qquad \text{(S2)}$$

$$\mathbf{2}•Cl^– + TBA^+ = \mathbf{2}•Cl^–•TBA^+ \qquad K_{ipc} \qquad \text{(S3)}$$

A free fit, where both K_a and K_{ipc} are allowed to float, generated unrealistic chemical shift values (see below). Therefore, to obtain accurate outcome to the fitting analysis, the value of K_a was systematically varied from 3.8 – 4.4 while K_{ipc} was optimized using the software. Each fitting result (Table S1) was examined and would be considered realistic only if all of the following conditions apply: (1) The generated chemical shift values of the aromatic protons (a-c) are in the range of $6.5 < \delta < 11.0$ ppm; (2) The generated chemical shift values of the aliphatic protons (d-e, α-CH_2) are in the range of $2.0 < \delta < 5.5$ ppm; (3) for each proton included in the fitting, the differences in the chemical shift positions between **2**•$Cl^–$ and **2**•$Cl^–$•TBA^+ are smaller than 1.0 ppm. The $Cl^–$ binding energy of triazolophane **2** was determined as $\log K_a = 4.1 \pm 0.2$ ($\Delta G_a = –23 \pm 2$ kJ mol$^{–1}$) on the basis of the three criteria used above. Similarly, the stability of the ion-pair complex was found to be $\log K_{ipc} = 3.6 \pm 0.2$ ($\Delta G_{ipc} = –21 \pm 2$ kJ mol$^{–1}$).

Table S1. Result of HypNMR2008 data fitting as the value of $\log K_a$ was systematically varied.

$\log K_a$	3.8	3.9	4.0	4.1	4.2	4.3	4.4	4.5[a]
$\log(K_a•K_{ipc})$	7.8	7.8	7.8	7.7	7.7	7.7	7.6	7.4[a]
$\log K_{ipc}$	4.0	3.9	3.8	3.6	3.5	3.4	3.2	2.9
Sigma[b]	4.5	3.9	3.2	2.6	2.0	1.5	1.1	1.0
Realistic?	no	no	partially	yes	yes	partially	no	no

a. Both $\log K_a$ and $\log(K_a•K_{ipc})$ are allowed to float. *b*. Sigma represents the residual of fitting. Smaller sigma values indicate a better match between the experimental and the calculated value.

Sample HypNMR2008 Output (*realistic* fitting):

Sigma = 2.61

	value	standard deviation
log beta(TCl)	4.86	fixed
log beta(MCl)	4.10	fixed
log beta(MClT)	7.74	0.01

Chemical shifts for each nucleus (error on 4th decimal place)

	M	T	TCl	MCl	MClT	Error
a	7.28			10.23	9.71	0.02
b	7.67			8.98	8.75	0.01
c	7.42			8.17	8.04	0.01
e	4.61			4.43	4.51	0.01
d	2.84			2.92	2.95	0.01
a-CH2-		3.08	3.34		3.15	0.01

Sample HypNMR2008 Output (*unrealistic* fitting):

Sigma = 0.98

	value	standard deviation
log beta(TCl)	4.86	fixed
log beta(MCl)	4.53	0.02
log beta(MClT)	7.42	0.04

Chemical shifts for each nucleus (error on 4th decimal place)

	M	T	TCl	MCl	MClT	Error
a	7.28			9.39	11.50	0.03
b	7.67			8.61	9.55	0.27
c	7.42			7.96	8.51	0.01
e	4.61			4.48	4.48	0.12
d	2.84			2.90	3.06	0.01
a-CH2-		3.13	3.33		3.11	0.07

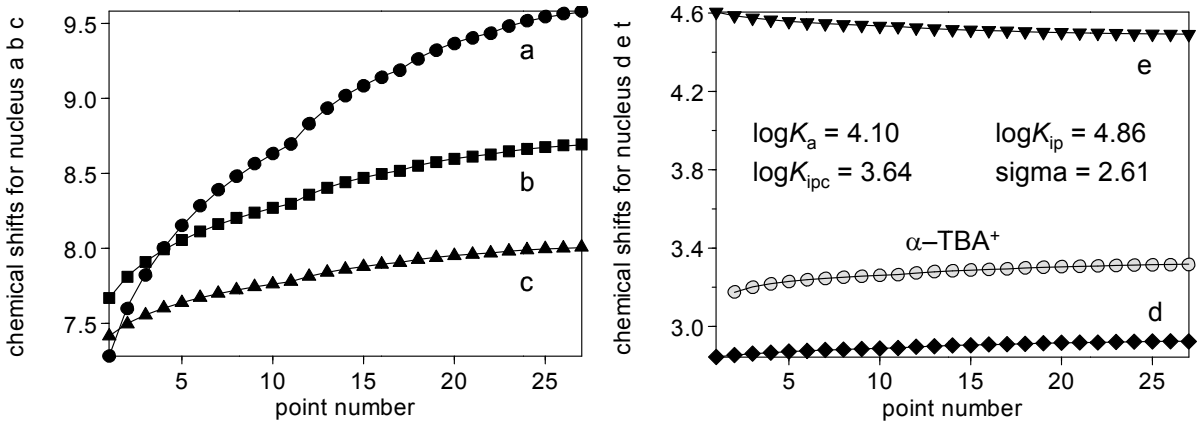

Figure S2. Results of data fitting using HypNMR2008 with three equilibria (Eq. S1−S3). Experimental chemical shift positions (symbols) are well reproduced by calculated values (lines).

S.5 ^{1}H NMR VARIABLE CONCENTRATION EXPERIMENT OF TRIAZOLOPHANE 2

Self-association can result in an incorrect evaluation of the diffusion coefficient of triazolophane **2**. Therefore, a variable concentration NMR experiment is performed to estimate the amount of multimers in solution.

Solutions containing triazolophane **2** in a range of concentrations (0.18 – 1.25 mM, CD_2Cl_2) were prepared and ^{1}H NMR spectra were recorded. The chemical shift of proton a was found to be independent of concentration (Figure S3). Simulating the data with an equal *K* model (Eq. S4)[S6] failed to generate the self-association constant.

$$\delta_{obs} = \delta_{aggregate} + \left(\delta_{aggregate} - \delta_{monomer}\right) \cdot \left(1 + \frac{1-\sqrt{1+4 \cdot c \cdot K_E}}{2 \cdot c \cdot K_E}\right) \qquad \text{(S4)}$$

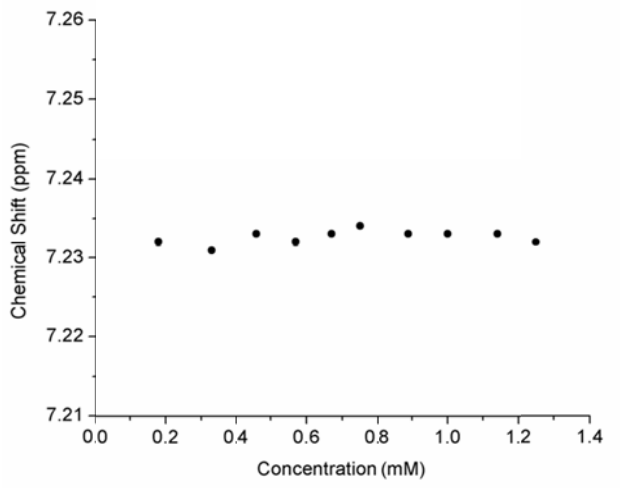

Figure S3. ^{1}H NMR variable concentration experiment of triazolophane **2** showing the peak position of proton a.

S.6 DIFFUSION NMR TITRATION OF TRIAZOLOPHANE 2

Solutions containing known amounts of triazolophane **2** and $TBA^+•Cl^-$ were prepared in a sealed NMR tube and PGSE NMR measurements were performed. The self-diffusion coefficients, *D*, of triazolophane protons (e and f) and tetrabutylammonium protons (the α-methylene and δ-methyl protons) were calculated (Table S2). In a solution containing triazolophane **2** and $TBA^+•Cl^-$ which exist in the presence of all three equilibria, the observed diffusion coefficient based on the triazolophane (Eq. S5) and TBA^+ (Eq. S6) signals can be represented as follows:

$$D_{t,obs}(\mathbf{2}) = D_t(\mathbf{2}) \times f(\mathbf{2}) + D_t(\mathbf{2}•Cl^-) \times f(\mathbf{2}•Cl^-) + D_t(\mathbf{2}•Cl^-•TBA^+) \times f(\mathbf{2}•Cl^-•TBA^+) \quad (S5)$$

$$D_{t,obs}(TBA^+) = D_t(TBA^+) \times f(TBA^+) + D_t(TBA^+•Cl^-) \times f(TBA^+•Cl^-) + D_t(\mathbf{2}•Cl^-•TBA^+) \times f(\mathbf{2}•Cl^-•TBA^+) \quad (S6)$$

Where is $D_{t,obs}(\mathbf{2})$ and $D_{t,obs}(TBA^+)$ are the observed self-diffusion coefficients based on triazolophane **2** and TBA^+, respectively. D_t is the self-diffusion coefficient of the species in interest, and the *f* value is the fraction number of species in interest as relative to the total population of the species that are in exchange with the species in interest.

The result of the dffusion NMR titration justifies the inclusion of the ion-pair complexation equilibrium (K_{ipc}, Eq. S3) in the binding model. The experimentally *observed* diffusion coeffecients of the small TBA^+ ccation from a solution of **2**:$TBA^+•Cl^-$ at 1:0.75 and 1:1.5 molar ratios ([**2**] = 1 mM, Table S2) were *smaller* than that of free TBA^+ and $TBA^+•Cl^-$ (i.e., 10.1±0.1 < 10.6±0.1). Thus, the only explanation that can rationalize these observations is that the the TBA^+ cation is involved in an equilibrium to form a larger species, i.e., the ion-pair complex $\mathbf{2}•Cl^-•TBA^+$.

The diffusion coefficient of **2** (8.1±0.2) was observed to get smaller (7.6±0.2) with increasing amounts of $TBA^+•Cl^-$ (Table S2). However, this observation is not as conclusive as the diffusion coefficient of TBA^+, on account of the fact that the diffusion coefficient of $\mathbf{2}•Cl^-$ is unknown.

Table S2. Diffusion coefficients ($\pm 0.1 \times 10^{-10}$ m^2 s^{-1}) generated from control and titration NMR experiments.

	TBA^+			Triazolophane **2**		
	H^α	H^δ	Ave.	H^e	H^f	Ave.
$TBA^+•Cl^-$			10.6			
TBA^+			10.6			
2[a]				7.9	8.3	8.1±0.2
2 + $TBA^+•Cl^-$ (0.75 equiv.)[b]	10.0	10.2	10.1	7.8	8.0	7.9
2 + $TBA^+•Cl^-$ (1.5 equiv.)[b]	9.9	10.0	10.0	7.4	7.7	7.6±0.2

a. [**2**] = 0.5 mM. *b*. [**2**] = 1 mM.

S.7 SIMULATED SPECIATION CURVES FOR CHLORID BINDING WITH TRIAZOLOPHANE 2

Speciation curves (Figure S4–S5) were calculated with HySS2006[S7] using the binding energies obtained from NMR titration. It can be suggested that:

(1) At the end of the ^{1}H NMR titration ([**2**] = 500 μM, 20 equivalents of $TBA^+ \bullet Cl^-$, Figure S4), over 90% of the receptors are complexed with Cl^-. Therefore, this titration was performed under conditions where the association constants obtained from the titration are accurate.[S8]

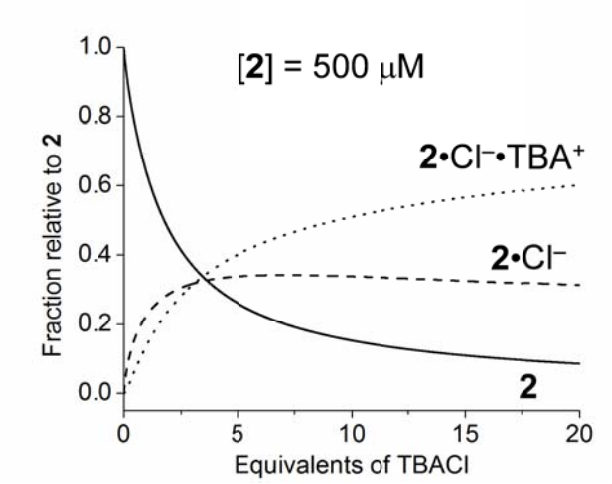

Figure S4. Simulated speciation curves at the corresponding NMR titration concentrations with triazolophane **2**. Association constants used: $\log K_a = 4.1$, $\log K_{ip} = 4.9$, $\log K_{ipc} = 3.6$.

(2) At the diffusion NMR titration condition ([**2**] = 1 mM, 0.75 ~ 1.5 equivalents of $TBA^+ \bullet Cl^-$, Figure S5b, S5d), a significant amount of TBA^+ cations (~20%) exist in the form of ion-pair complex **2**•Cl^-•TBA^+. This distribution of species matches the lowered diffusion coefficients observed experimentally for the TBA^+ cation.

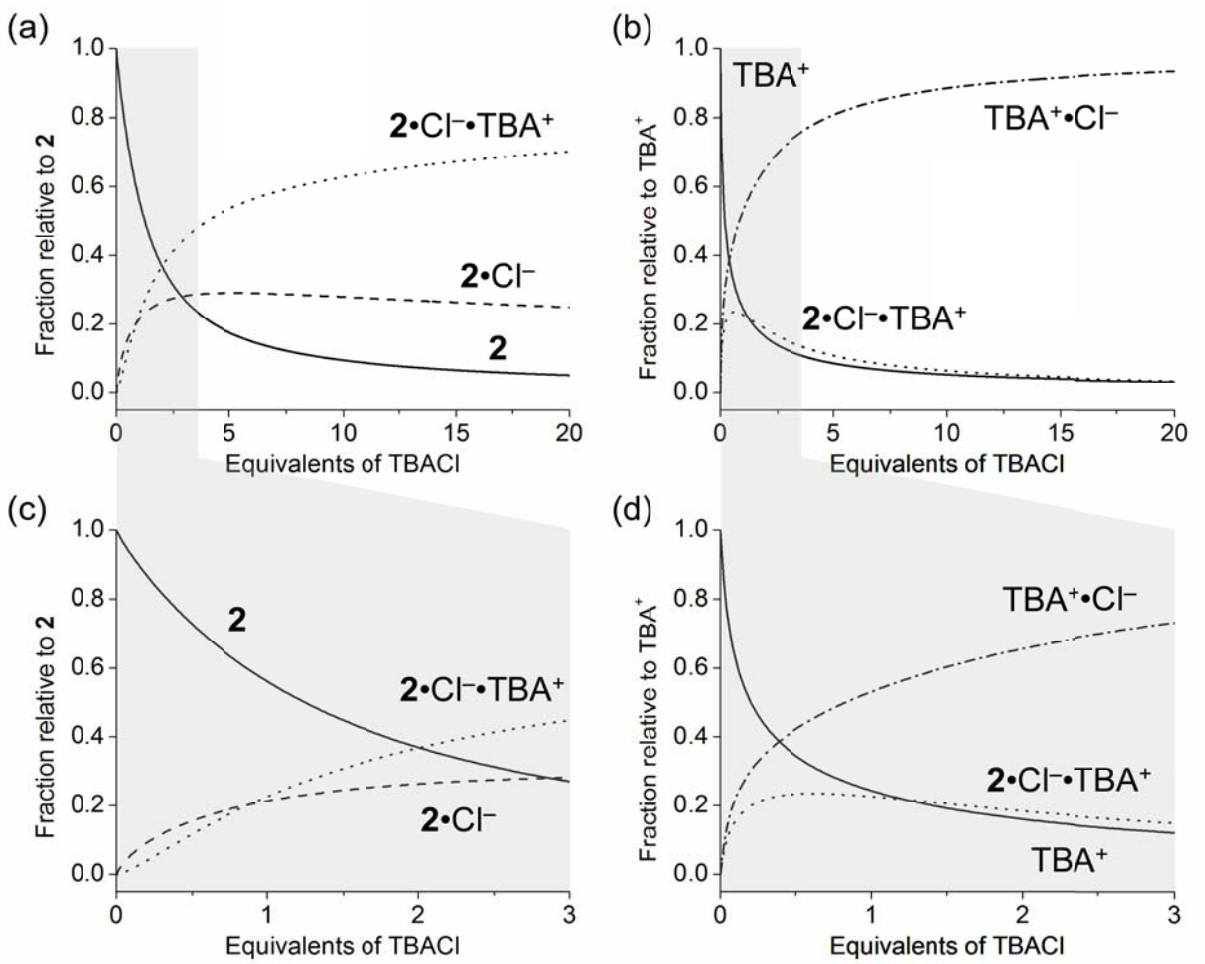

Figure S5. Simulated speciation curves at the diffusion NMR titration concentration (1 mM) as a fraction related to receptor **2** (left) and to TBA^+ cation (right). Association constants used: $\log K_a = 4.1$, $\log K_{ip} = 4.9$, $\log K_{ipc} = 3.6$.

S.8 CHLORIDE BINDING ENERGY OF OLIGOMER 3

The previously published[S9] titration data of oligomer **3** was reinvestigated using the complete set of binding equilibria that are now known to be important (Eq. S1–S3). Chemical shift migrations of protons a, b, h (Figure S6) were modeled by HypNMR2008. When all three equilibria (Eq. S1–S3) were included, the data fitting did not converge. Instead, a successful fitting could only be obtained using Eq. S2 and S7. The overall stability of the ion-pair complex was determined to be $\log\beta_{ipc} = \log(K_a \times K_{ipc}) = 5.7 \pm 0.1$.

$$TBA^+ + Cl^- = TBA^+ \bullet Cl^- \qquad K_{ip} \qquad \text{(S2)}$$

$$\mathbf{3} + TBA^+ + Cl^- = \mathbf{3} \bullet Cl^- \bullet TBA^+ \qquad \beta_{ipc} = K_a \times K_{ipc} \qquad \text{(S7)}$$

The chloride affinity of oligomer **3** can be estimated by assuming that the affinity of the anionic complex **3**•Cl^- for the cation TBA^+ is the same as **2**•Cl^- ($\log K_{ipc} = 3.8$). Therefore, the $\log K_a$ value of oligomer **3** can be calculated: $\log K_a = \log\beta_{ipc} - \log K_{ipc} = 1.9 \pm 0.3$ ($\Delta G_a = 11 \pm 2$ kJ mol^{-1}).

A simulated speciation curve (Figure S7) at the concentration used in the NMR titration (10 mM, see below) suggested that the 1:1 binding of oligomer **3** (Eq. S1) is so weak that less than 5% of the complex exists in the form of **3**•Cl^- at any stage throughout the titration. Instead, the ion-pair complex **3**•Cl^-•TBA^+ is the major species with increasing equivalent of TBA^+•Cl^-. Consequently, only estimates of K_a and K_{ipc} could be obtained under this experimental condition.

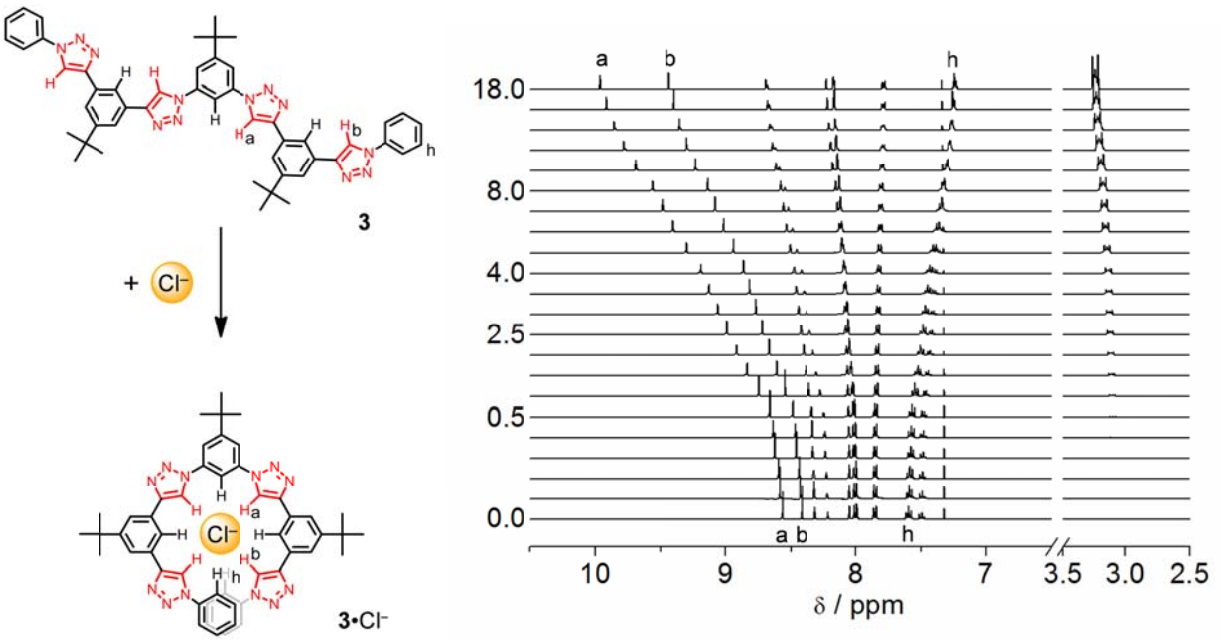

Figure S6. Partial ^{1}H NMR spectra of oligomer **3** (10 mM, CD_2Cl_2, 298 K) recorded upon titration with TBA^+•Cl^- (0–18 equivalents).

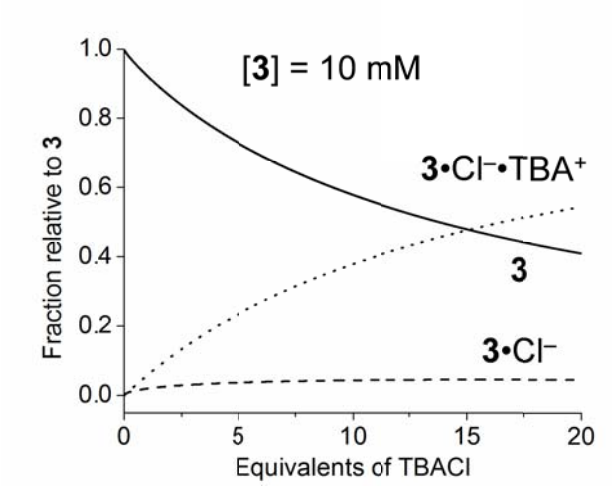

Figure S7. Simulated speciation curves at the corresponding NMR titration concentrations with oligomer **3**. Association constants used: $\log K_a = 1.9$, $\log K_{ip} = 4.9$, $\log K_{ipc} = 3.8$.

S.9 ESTIMATING THE DEFORMATION ENERGIES, NET CHLORIDE BINDING ENERGIES TO THE RECEPTORS AND INDIVIDUAL CH•••Cl⁻ HYDROGEN BONDS

The chloride binding process can be deconvoluted to two separate reactions – preparing the correct conformer and binding chloride to the correct conformer. The equilibria for triazolophane **1** are exemplary:

1 = **1***	+10 kJ mol^{-1}	Preparing the correct the conformation	(S8)
1* + Cl$^-$ = **1**•Cl$^-$	–48 kJ mol^{-1}	Chloride binding to the conformation	(S9)
1 + Cl$^-$ = **1**•Cl$^-$	–38 kJ mol^{-1}	Overall reaction quantified	(S10)

Assuming the deformation energy (ΔG(S8)) required to prepare the correct conformation **1*** in our solution studies is equal to the one we calculated in the gas phase (+10 kJ mol^{-1}),[S10] the binding energy to the perfectly organized macrocycle is estimated as: ΔG(S9) = ΔG(S10) – ΔG(S8) = –48 kJ mol^{-1}.

We can then use this value (ΔG(S9) = −48 kJ mol^{-1}) and our knowledge from computations that the relative strength of the triazole CH (T), the N-linked phenylene CH (N), and the C-linked phenylene CH (C): T : N : C = 10 : 4 : 3. According to this ratio, in parent triazolophane **1** (ΔG(S9) = –48 kJ mol^{-1}), the free energy contribution from each triazole CH, N-linked phenylene CH, C-linked CH is calculated to be −8.9, −3.6, and −2.7 kJ mol^{-1}, respectively. From Hay,[S11] we also know that one methylene CH is about half the strength of a phenyl CH. Therefore, in the flexible triazolophane **2**, each propylene CH would contribute −1.3 kJ mol^{-1} in binding energy.

Overall, the net chloride binding energies for receptor **2** (Eq. S12, where two N-linked phenylenes are substituted by two propylenes) and **3** (Eq. S15, where one extra N-linked

phenylene is present) are calculated (Table S3). The corresponding deformation energy for receptor **2** (Eq. S11) and **3** (Eq. S14) can also be estimated.

2 = **2*** (S11) $\Delta G = -23 - (-44.4) = 21.4$ kJ mol^{-1}
2* + Cl$^-$ = **2**•Cl$^-$ (S12) $\Delta G = -48 - 2 \times (-3.6) + 2 \times (-1.3) = -44.4$ kJ mol^{-1}
2 + Cl$^-$ = **2**•Cl$^-$ (S13) $\Delta G = -23$ kJ mol^{-1}

3 = **3*** (S14) $\Delta G = -11 - (-51.6) = 40.6$ kJ mol^{-1}
3* + Cl$^-$ = **3**•Cl$^-$ (S15) $\Delta G = -48 + -3.6 = -51.6$ kJ mol^{-1}
3 + Cl$^-$ = **3**•Cl$^-$ (S16) $\Delta G = -11$ kJ mol^{-1}

Table S3. Expected net chloride binding energy and the fee energy contribution from each types of donors.

Unit: kJ mol^{-1}	H-bond strength of single donor	**1**	**2**	**3**
Triazole CH	–8.9	–8.9 × 4 = –35.6	–8.9 × 4 = –35.6	–8.9 × 4 = –35.6
N-linked Ph CH	–3.6	–3.6 × 2 = –7.2		–3.6 × 3 = –10.8
C-linked Ph CH	–2.7	–2.7 × 2 = –5.4	–2.7 × 2 = –5.4	–2.7 × 2 = –5.4
Methylene CH	–1.3		–1.3 × 2 = –2.6	
Expected Δ*G*		**–48**	**–44**	**–52**
Observed Δ*G*		**–38**	**–23**	**–11**

The contribution from each type of pre-organization can be quantified by comparing the appropriate deformation free energies:

Macrocyclic effects:
Benefit of the highly pre-organized macrocycle **1** compared to poorly pre-organized oligomer **3**
$\Delta G(1) - \Delta G(7) = 10 - 41 = -31$ kJ mol^{-1}

Benefit of the partially pre-organized macrocycle **2** compared to poorly pre-organized oligomer **3**
$\Delta G(4) - \Delta G(7) = 21 - 41 = -20$ kJ mol^{-1}

Conformational Pre-organization (aka rigidity)
Benefit of highly pre-organizing the macrocycle **1** compared to **2**
$\Delta G(1) - \Delta G(4) = 10 - 21 = -11$ kJ mol^{-1}

S.10 GENERAL COMPUTATIONAL METHODS

Density functional theory (DFT) calculations in the gas phase have been carried out using the *Gaussian 03*[S12] suite of programs. All the geometries have been optimized and the single point energies were obtained using the standard B3LYP[S13] density functional. The 6-31+G(d,p) basis set was used throughout. The deformation energy was defined as the energy difference between the lowest energy conformation of $\mathbf{2}^{\#}$ and the conformation of $\mathbf{2}^{\#}$ in the chloride complex but with the chloride removed.

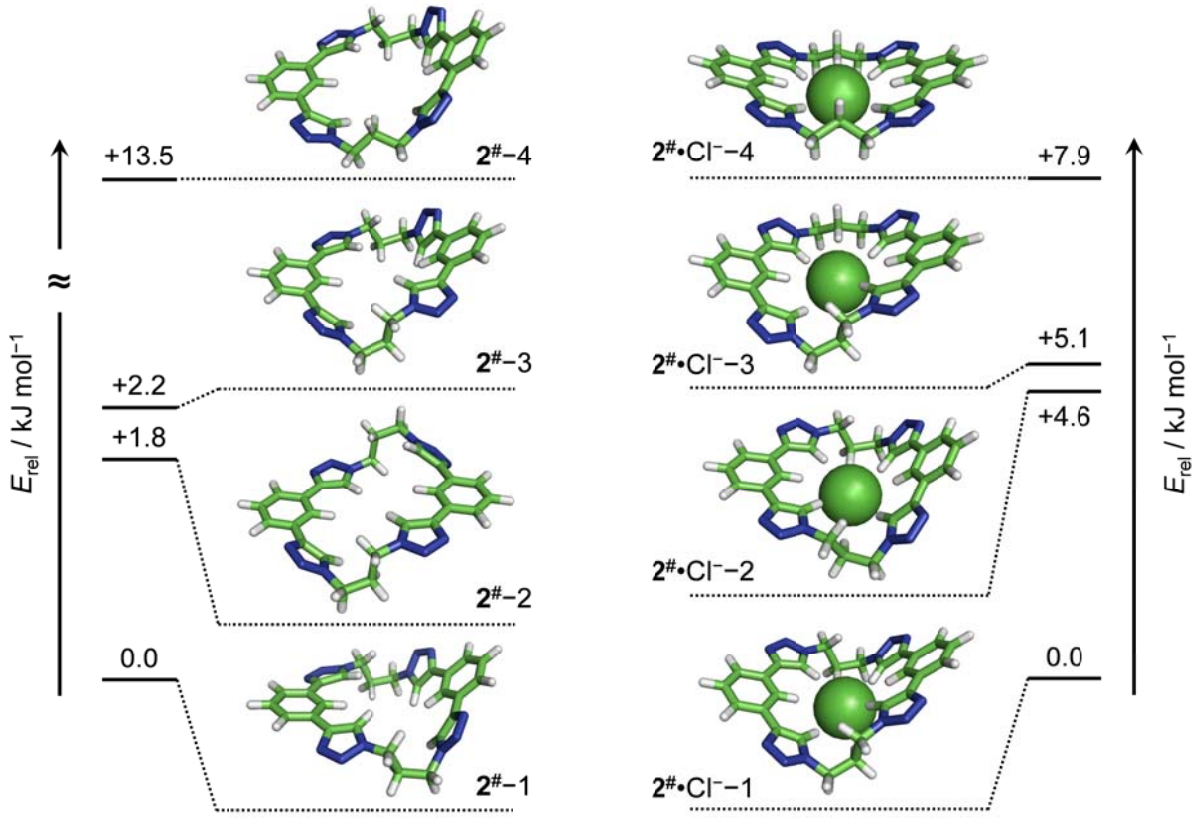

Figure S8. Optimized geometries and relative energies (kJ mol^{-1}) of the low energy conformations of triazolophane $\mathbf{2}^{\#}$ and its chloride complexes (B3LYP / 6-31+G(d,p)).

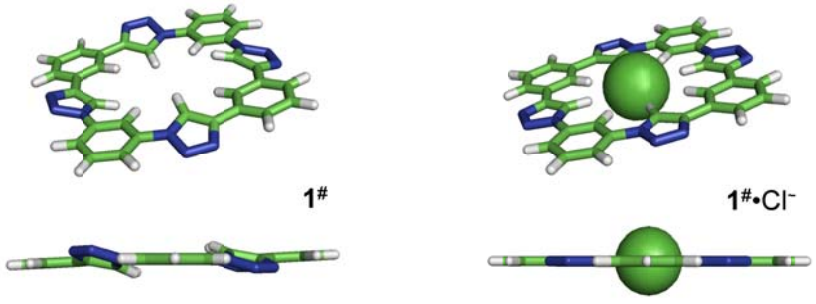

Figure S9. Optimized geometries of $\mathbf{1}^{\#}$ and its chloride complex (B3LYP / 6-31+G(d,p)).

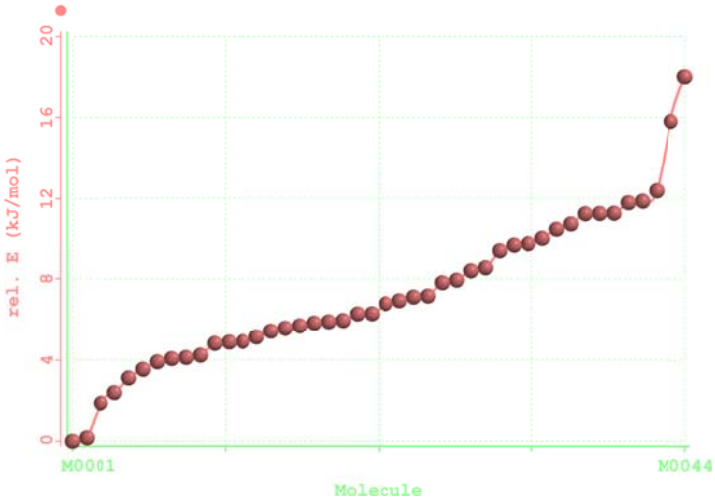

Figure S10. Conformational space of free oligomer **3** (AM1).

S.11 EVALUATION OF ELECTROSTATIC REPULSIONS

The distances between inward facing hydrogen atoms ($d_{H\cdots H}$) are obtained from the calculated structures of $\mathbf{1}^{\#}$ and its complex $\mathbf{1}^{\#}\bullet Cl^{-S10}$ and $\mathbf{2}^{\#}$ and $\mathbf{2}^{\#}\bullet Cl^{-}$ discussed here. Three types of $d_{H\cdots H}$, between adjacent triazole-phenylene, adjacent triazole-triazole, and diagonal triazole-triazole, have been measured in all the low energy conformations of the two macrocycles (Table S4).

Table S4. Hydrogen-hydrogen distances ($d_{H\cdots H}$, Å) measured in the two macrocycles ($\mathbf{1}^{\#}$ and $\mathbf{2}^{\#}$) and their chloride complexes ($\mathbf{1}^{\#}\bullet\mathbf{Cl}^{-}$ and $\mathbf{2}^{\#}\bullet\mathbf{Cl}^{-}$).

	$\mathbf{1}^{\#}$	$\mathbf{1}^{\#}\bullet Cl^{-}$	$\mathbf{2}^{\#}$	$\mathbf{2}^{\#}\bullet Cl^{-}$
Adjacent triazole-phenylene	2.30	2.16	2.53	2.27
Adjacent triazole-triazole	4.00	3.72	4.23	3.56
Diagonal triazole-triazole	5.66	5.26	5.99	4.80

S.12 ELECTROSTATIC POTENTIALS

Electrostatic potential (ESP) energy surface calculations were carried out at HF/3−21G level of theory using the fully optimized geometries. Compared to the free macrocycle $\mathbf{1}^{\#}$ and $\mathbf{2}^{\#}$ (Figure S9), the electrostatic potential of the binding cavity became more positive in their corresponding chloride binding conformation $\mathbf{1}^{\#*}$ and $\mathbf{2}^{\#*}$, indicating an increased electrostatic repulsion resulted by bringing the CH donors together. The energies required to overcome this increased repulsion is believed to be the major source of the preparation penalty.

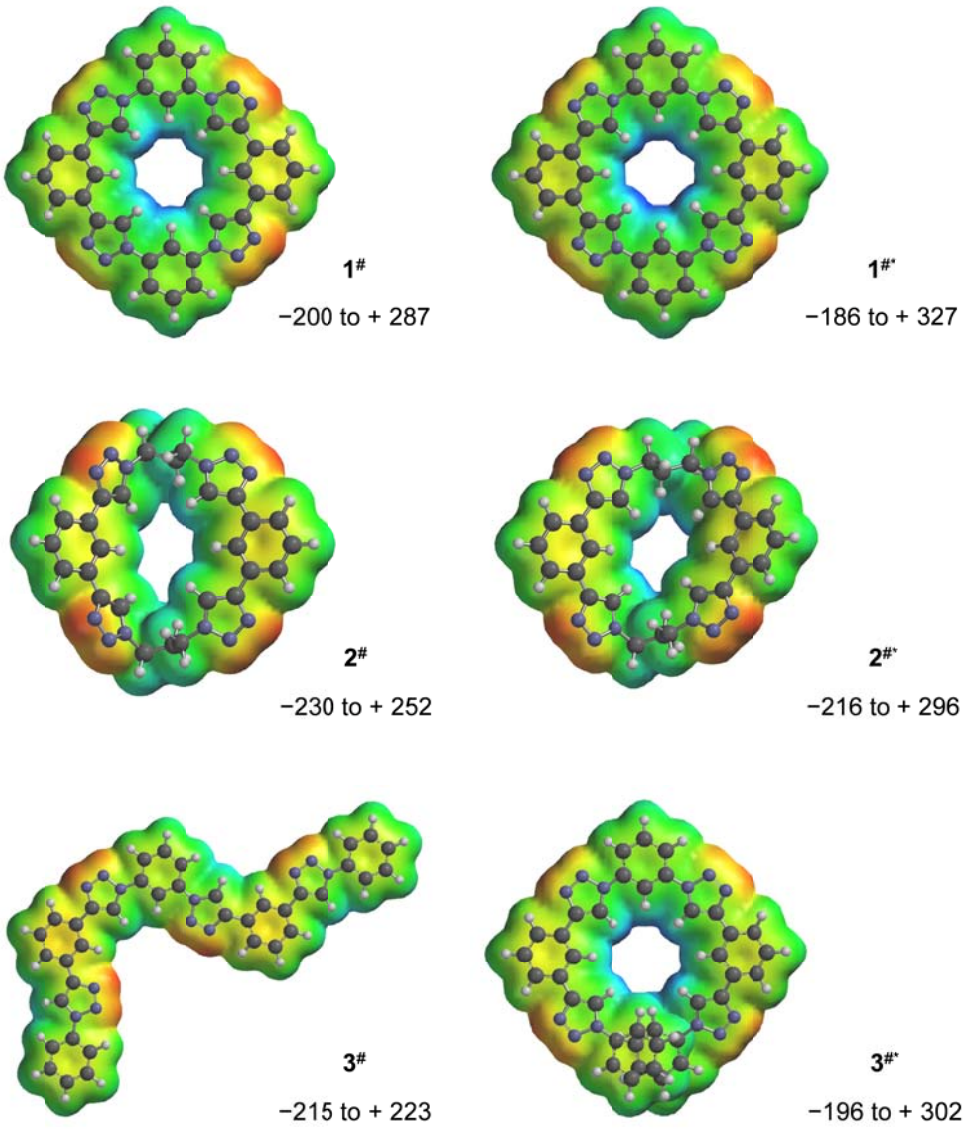

Figure S11. Electrostatic potential energy surfaces (kJ mol^{-1}) calculated for the free receptors (**1**$^{\#}$, **2**$^{\#}$, and **3**$^{\#}$) and their optimal chloride binding conformations (**1**$^{\#*}$, **2**$^{\#*}$, and **3**$^{\#*}$). ESP: −230 (red) to 330 (blue) ev.

S.13 ESTIMATING THE SOLVENT ACCESSIBILITY OF THE CHLORIDE COMPLEXES

The solvent accessible areas of the three chloride complexes are expected to be similar by inspecting the optimized geometries (Figure S12). Compared with the **1**•Cl^{-} complex, the chloride ion in complex **2**•Cl^{-} is more exposed to solvent on one side, while less exposed on the

other. Overall, **2**•Cl^- might be slightly better solvated than **1**•Cl^-. A similar opening and closing effect is also present in **3**•Cl^-.

Figure S12. Side view of the optimized geometries of the three chloride complexes. Solvent accessible areas are marked in light blue.

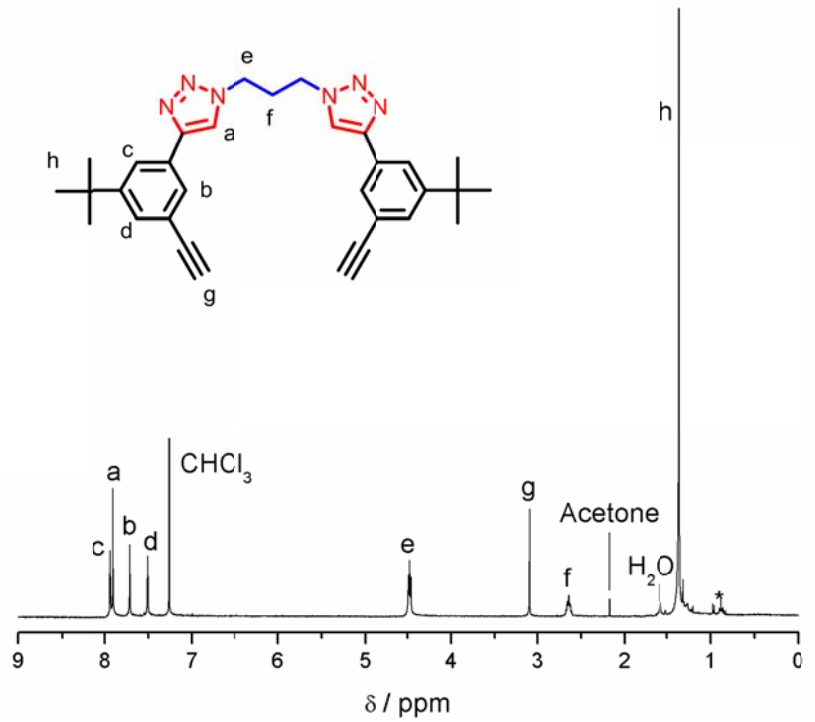
e
f
a
c
h
b
d
g
h
a
CHCl3
c
b
d
e
g
Acetone
f
H2O
9
8
7
6
5
4
3
2
1
0
δ / ppm

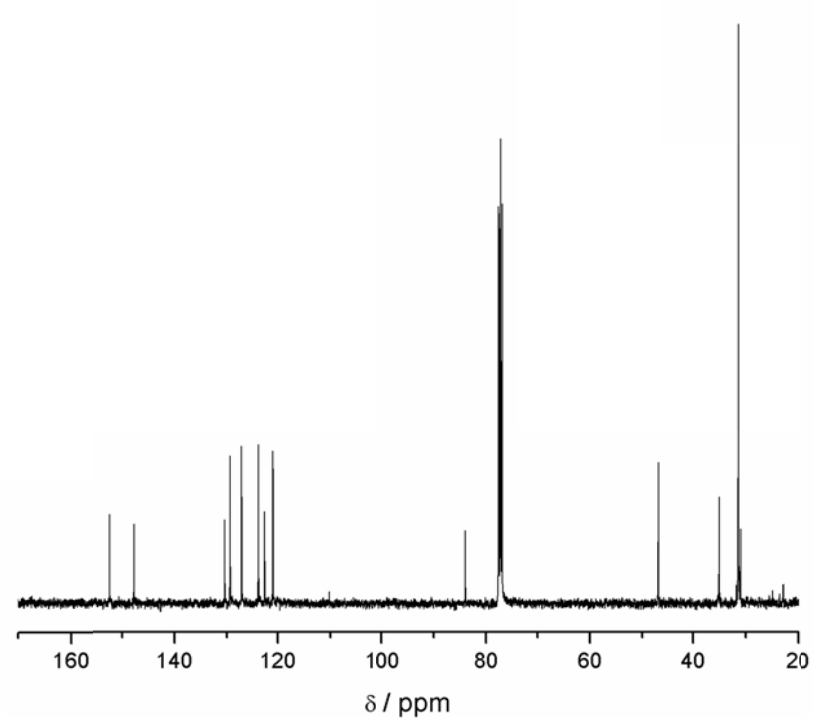
160
140
120
100
80
60
40
20
δ / ppm

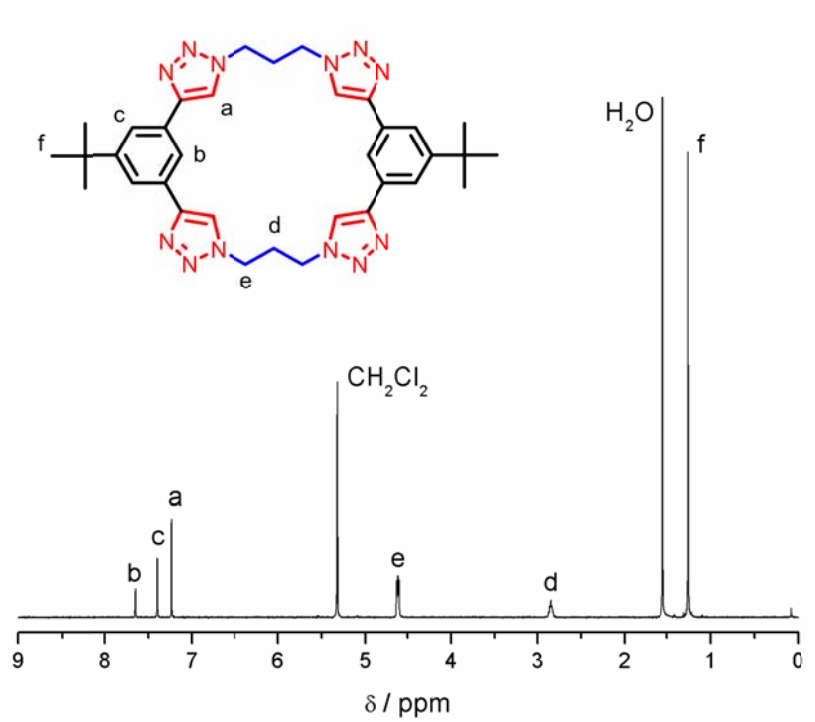
a
b
c
d
e
f
H2O
CH2Cl2
9
8
7
6
5
4
3
2
1
0
δ / ppm

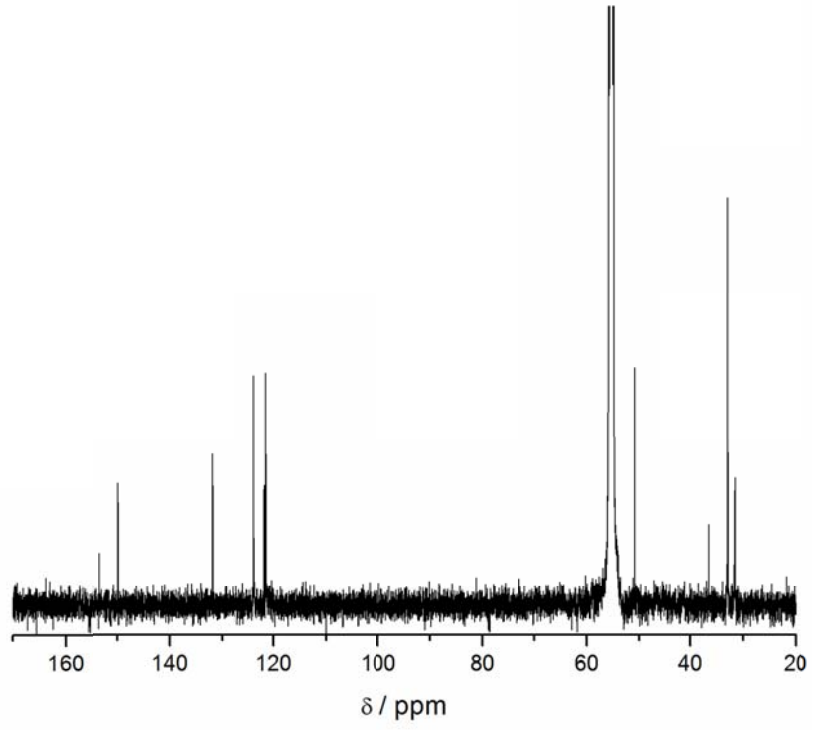
160
140
120
100
80
60
40
20
δ / ppm

Reference

S1 M. D. LoCoco, X. Zhang, and R. F. Jordan, *J. Am. Chem. Soc.* 2004, **126**, 15231–15244.

S2 Y. Hua, R. O. Ramabhadran, E. O. Uduehi, J. A. Karty, K. Raghavachari and A. H. Flood, *Chem. Eur. J.* 2011, **17**, 312–321.

S3 C. Frassineti, S. Ghelli, P. Gans, A. Sabatina, M. S. Moruzzi, and A. Vacca, *Anal. Biochem.* 1995, **231**, 374–382.

S4 A low intensity peak corresponding to the m/z of $\mathbf{2}_2$•Cl^- complex was seen from ESI-MS titration (Figure S1), whereas no feature of 2:1 complex was identified with ^{1}H NMR and diffusion NMR titration. Attempting to include the 2:1 equilibrium into data fitting generated erroneous results. The 2:1 binding equilibrium was therefore not included, on account of the fact that the sandwich complex was only seen in the gas phase.

S5 S. Alunni, A. Pero, and G. J. Reichenbach, *J. Chem. Soc., Perkin Trans. 2* 1998, 1747–1750.

S6 R. B. Martin, *Chem. Rev.* 1996, **96**, 3043–3064.

S7 L. Alderighi, P. Gans, A. Ienco, D. Peters, A. Sabatini, and A. Vacca, *Coord. Chem. Rev.* 1999, **184**, 311–318.

S8 K. Hirose, in Analytical Methods in Supramolecular Chemistry, (Eds: C. A. Schalley), Wiley-VCH, 2007.

S9 Y. Li and A. H. Flood, *J. Am. Chem. Soc.* 2008, **130**, 12111–12122.

S10 I. Bandyopadhyay, K. Raghavachari and A. H. Flood, *ChemPhysChem* 2009, **10**, 2535–2540.

S11 L. Pedzisa and B. P. Hay, *J. Org. Chem.* 2009, **74**, 2554−2560.

S12 (a) M. J. Frisch, *et al.* Gaussian *03*, Gaussian, Inc.: Wallingford, CT, 2004; (b) M. J. Frisch, *et al.* Gaussian *09*, Gaussian, Inc.: Wallingford, CT, 2009.

S13 (a) C. Lee, W. Yang, and R. G. Parr, *Phys. Rev. B* 1988, **37**, 785–789; (b) A. D. Becke, *J. Chem. Phys.* 1993, **98**, 5648–5652.